Topological susceptibility with the improved Asqtad action

Claude Bernard
Department of Physics, Washington University, St. Louis, Missouri 63130, USA

Thomas DeGrand and Anna Hasenfratz
Physics Department, University of Colorado, Boulder, Colorado 80309, USA

Carleton DeTar and James Osborn
Physics Department, University of Utah, Salt Lake City, Utah 84112, USA

Steven Gottlieb
Department of Physics, Indiana University, Bloomington, Indiana 47405, USA

Eric Gregory and Doug Toussaint
Department of Physics, University of Arizona, Tucson, Arizona 85721, USA

Alistair Hart
School of Physics, University of Edinburgh, King's Buildings, Edinburgh EH9 3JZ, United Kingdom

Urs M. Heller
American Physical Society, One Research Road, Box 9000, Ridge, New York 11961, USA

James Hetrick
Physics Department, University of the Pacific, Stockton, California 95211, USA

Robert L. Sugar
Department of Physics, University of California, Santa Barbara, California 93106, USA
(Received 20 August 2003; published 3 December 2003)

Chiral perturbation theory predicts that in quantum chromodynamics light dynamical quarks suppress the topological (instanton) susceptibility. We investigate this suppression through direct numerical simulation using the Asqtad improved lattice fermion action. This action holds promise for carrying out nonperturbative simulations over a range of quark masses for which chiral perturbation theory is expected to converge. To test the effectiveness of the action in capturing instanton physics, we measure the topological susceptibility as a function of quark masses with $2+1$ dynamical flavors. Our results, when extrapolated to zero lattice spacing, are consistent with predictions of leading order chiral perturbation theory. Included in our study is a comparison of three methods for analyzing the topological susceptibility: (1) the Boulder hypercubic blocking technique with the Boulder topological charge operator, (2) the more traditional Wilson cooling method with the twisted plaquette topological charge operator and (3) the improved cooling method of de Forcrand, Perez, and Stamatescu and their improved topological charge operator. We show in one comparison at nonzero lattice spacing that the largest difference between methods (1) and (2) can be attributed to the operator, rather than the smoothing method.

DOI: 10.1103/PhysRevD.68.114501 PACS number(s): 11.15.Ha, 12.38.Aw, 12.38.Gc, 12.39.Fe

I. INTRODUCTION

Chiral perturbation theory predicts the behavior of the topological susceptibility in the limit of small quark mass. For improved fermion actions such as Asqtad [1] that lack complete chiral symmetry at nonzero lattice spacing, reproducing this prediction is a particularly challenging test.

The Asqtad improvement adds local three-, five-, and seven-link terms to the standard staggered fermion action to eliminate tree-level lattice artifacts to order a^2 [1]. Here we use it in conjunction with the one-loop improved Symanzik gauge action. This action has proven to be highly successful in determining the masses of the light hadrons [2] and a variety of quarkonium masses and meson decay parameters [3]. It appears that the most satisfactory agreement with experimental values is achieved so far for those quantities that are well behaved in the chiral limit.

Whether improvement is successful in reducing lattice artifacts clearly depends on the observable. The Asqtad quark-gluon vertex is not as smooth as that of the more elaborate hyperrubic (HYP) action [4] and zero modes are not treated as rigorously as with the more expensive domain wall and overlap actions [5,6]. Through a rougher vertex, quark propagation might be influenced by small instantonlike dislocations. With imprecise zero modes, at small quark mass the fermion determinant may fail to suppress adequately configurations with nonzero topological charge.

The gluonic measurement of topological charge by summing the charge density is sensitive to the choice of both the discretization of the charge density operator and the smoothing or cooling method. Consequently, we found it instructive to compare three methods for measuring the charge:

(1) The Boulder definition of the topological charge density [7] with smoothing through hypercubic blocking [8].

(2) The more traditional combination of measuring the charge density through the twisted plaquette operator and cooling by minimizing the Wilson action [9,10].

(3) Measuring the charge density with the five-loop improved operator and cooling with a five-loop improved gauge action [11].

Throughout, we shall abbreviate these methods with ''Boulder/HYP,'' ''TwPlaq/Wilson,'' and ''5Li/5Li,'' respectively.

No previous study of the topological susceptibility has shown satisfactory agreement with the predictions of chiral perturbation theory at quark masses much smaller than the strange quark mass. Until recently [12–14], even the expected suppression of the susceptibility at small dynamical quark mass has been difficult to detect [15,16]. We argue that a combination of improvements in the lattice action, the smoothing (cooling) technique, the topological charge operator, and an $O(a^2)$ extrapolation to the continuum lead to plausible agreement with lowest order chiral perturbation theory for small quark masses.

This article is organized as follows. In Sec. II we introduce notation and review the predictions of chiral perturbation theory. Three methods for measuring the topological charge are compared and discussed in Sec. III. Results are presented in Sec. IV and discussed in Sec. V and conclusions are given in Sec. VI.

Preliminary results of this study were reported at Lattice 2002 Conference [17].

II. TOPOLOGICAL SUSCEPTIBILITY

The topological charge Q is the integral of the topological charge density ρ, which is in turn defined in terms of the Euclidean color gauge field $F^a_{\mu\nu}$ and its dual $\tilde{F}^a_{\mu\nu}$, through

$$Q=\int \rho d^4x=\frac{1}{32\pi^2}\int F^a_{\mu\nu}\tilde{F}^a_{\mu\nu}d^4x. \tag{1}$$

On a lattice of Euclidean space-time volume V the topological susceptibility is the mean fluctuation in the topological charge,

$$\chi=\frac{\langle Q^2\rangle}{V}. \tag{2}$$

Chiral perturbation theory predicts [18,19] that at large $\langle Q^2\rangle$ (i.e. large values of $mV\Sigma$, the product of the lightest quark mass, the lattice volume, and the chiral condensate parameter), and at sufficiently small quark masses, the topological susceptibility is related to the quark masses through

$$\chi=\frac{\Sigma}{(1/m_u+1/m_d+1/m_s)}. \tag{3}$$

For three flavors with $m_u=m_d=m_{u,d}$ we may use the partial conservation of the axial current (PCAC) relation between the up and down quark mass, pion decay constant, and the chiral condensate to write the susceptibility as

$$\chi=\frac{f_\pi^2 m_\pi^2}{4(1+m_{u,d}/2m_s)}, \tag{4}$$

showing that it vanishes linearly in the square of the pion mass in the chiral limit.

At infinite quark mass (lattice quenched approximation) the susceptibility is finite, requiring negative curvature corrections in Eq. (4), leading asymptotically to a constant [14,19,20]. Chiral perturbation theory, however, is not expected to converge for masses greater than m_s, so it provides no guidance there.

We test Eq. (4) against our measured susceptibility, pion mass [21], and pion decay constant [3] over a range of light quark masses.

III. MEASURING THE TOPOLOGICAL CHARGE ON THE LATTICE

In this section we compare three methods for measuring the topological charge. All three methods first smooth out ultraviolet fluctuations and then measure the topological charge density with a local discretized operator. All are equivalent in the continuum limit. However, some perform better at nonzero lattice spacing. To understand the comparison it is first useful to briefly review the effects of discretization on the topological susceptibility.

A. Discretization effects

The topological susceptibility measured on the lattice differs from the continuum value because of discretization errors in the measurement process and in the lattice action itself. The principal errors introduced in the measurement process are these:

(1) Instantons with a core size of the order of or less than the lattice spacing are excluded altogether.

(2) Small instantons shrink and are erased by prolonged smoothing.

(3) Intermediate sized instantons have a topological charge less than unity, owing to the discretization of the charge density operator.

(4) There are ''dislocations'' on the lattice: ultraviolet fluctuations that masquerade as topological charges.

The principal errors introduced by the action are these:

(1) For unquenched gauge configurations the staggered Dirac matrix has inexact zero modes so fails to fully ''see'' and suppress topological fluctuations adequately.

(2) Lattice artifact flavor (taste) symmetry breaking fails to account for light quark flavors correctly.

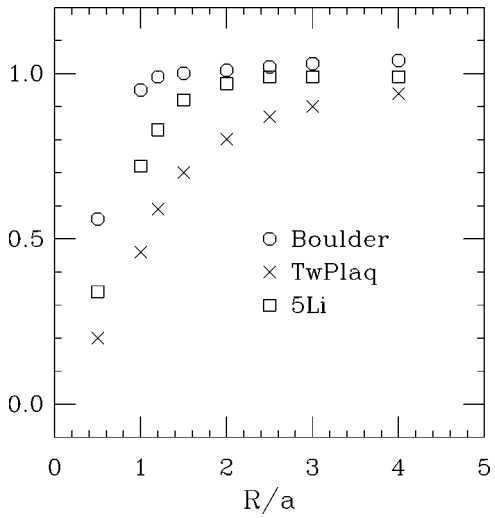

FIG. 1. Topological charge on artificial single instanton configurations as a function of instanton radius, comparing three observables: the traditional twisted plaquette operator, the Boulder operator [7] and the 5Li operator [11].

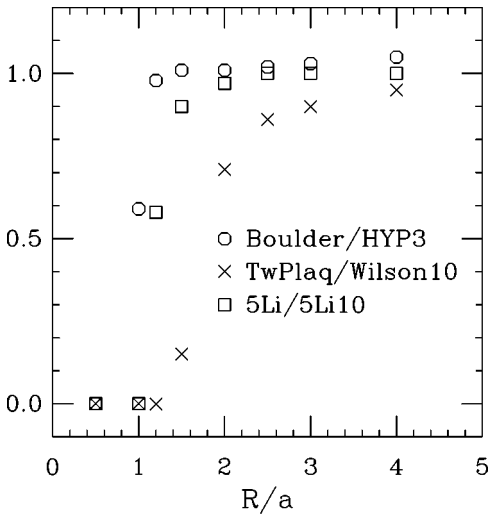

FIG. 2. Same as Fig. 1, but after smoothing.

B. Comparison of operators and smoothing methods

We consider the following topological charge density operators.

(1) TwPlaq: The original twisted plaquette operator, defined as an eight-link path with a displacement sequence $\{x,y,-x,-y,z,t,-z,-t\}$ plus rotations.

(2) 5Li: The five-loop improved operator of de Forcrand, Perez, and Stamatescu [11], built from a linear combination of five operators in the form of the twisted plaquette, but with the plaquettes replaced by various $m\times n$ rectangular Wilson loops.

(3) Boulder: The lattice approximation developed for SU(2) by DeGrand, Hasenfratz, and Kovacs [7] and refined for SU(3) by Hasenfratz and Nieter [22]. It involves a combination of two contorted Wilson loop operators in the fundamental and adjoint representations of SU(3), both defined on closed ten-link paths described by unit lattice vector displacements in the sequence $\{x,y,z,-y,-x,t,x,-t,-x,-z\}$ and $\{x,y,z,-x,t,-z,x,-t,-x,-y\}$ plus rotations and cyclic permutations. This operator was optimized to reduce lattice corrections for small instantons with radii close to the lattice spacing $R\approx a$.

All three operators are equivalent in the continuum limit, but they are subject to different discretization effects. Reference [23] makes a comparison of methods 2 and 3.

We first investigate how these operators perform with artificial instantons. We created a series of gauge configurations containing a single instanton of varying radius and measured the topological charge with each operator. Results are plotted in Fig. 1. As expected [7] the twisted plaquette operator tends to underestimate the topological charge for small instantons. The 5Li operator does better. The optimization of the Boulder operator is apparent.

Traditional cooling methods include minimizing the Wilson action [10] and minimizing improved actions, such as the 5Li action [11], that provide better scaling as a function of instanton radius, so are less likely to erase small instantons. Minimization is done through a series of standard heat-bath updates (cooling sweeps) at small gauge coupling. Hypercubic smoothing [8] was designed to be gentle and local so as to produce a smooth configuration with minimal distortion of the topology [24]. The smoothing process involves a series of APE blocking steps [25], constrained to lie entirely inside the hypercubes connected to the link being smoothed. We use the smoothing coefficients optimized in Ref. [22].

To see how cooling or smoothing affects the artificial instantons, we processed them using these methods. For the twisted plaquette operator we cooled with ten Wilson gauge action updates, for the 5Li operator ten 5Li updates. For the Boulder operator we smoothed with three hypercubic blocking sweeps. The number of smoothing steps in each case was chosen for stability of χ under further smoothing, as we shall discuss below. Results are shown in Fig. 2. It is evident that small instantons preserve their topological charge best with the Boulder/HYP method.

Next, we examine how the three methods perform on one of the gauge ensembles in our study, namely, the $20^3\times 64$ $a=0.12$ fm set with quark masses $am_{u,d}=0.01$ and $am_s=0.05$ [27]. We measured the topological susceptibility as a function of cooling or smoothing step and compared the results in Fig. 3. We see that it is reasonable to read off the Boulder/HYP susceptibility after three HYP sweeps and the TwPlaq/Wilson and 5Li/5Li susceptibilities after ten cooling sweeps. We made these arbitrary choices in an effort to compromise between preserving small instantons and reaching stability in the observable. We have tested these choices in a few cases, and find within statistical errors that our results are insensitive to increasing these values by a factor of 2 or 3. See also Ref. [23].

It is clear that at this lattice spacing the TwPlaq/Wilson method gives a lower susceptibility than the other methods. The 5Li/5Li result is closer to but still lower than the Boulder/HYP result. To determine the extent to which the difference in TwPlaq/Wilson is attributable to the observable and to the cooling method, we also measured the TwPlaq susceptibility on HYP smoothed lattices. The result (TwPlaq/HYP) shown in Fig. 3 is quite close to the TwPlaq/

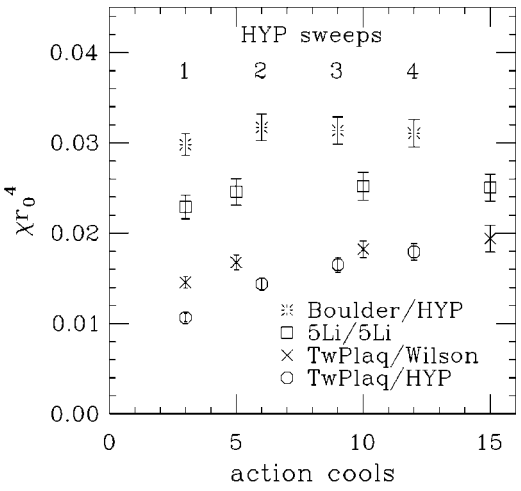

FIG. 3. Topological susceptibility as a function of smoothing or cooling step on the $20^3\times64$ dataset with $am_{u,d}=0.01$ and $am_s=0.05$, comparing four techniques: the Boulder topological charge operator with HYP smoothing [8], the twisted plaquette operator [9] with both Wilson action cooling [10] and HYP smoothing, and the 5Li operator with 5Li cooling [11]. (Results are expressed in units of r_0, the Sommer parameter [26].) The arbitrary scale conversion counts three cooling steps for one HYP smoothing sweep. Susceptibilities are measured on subvolumes as explained in Sec. IV.

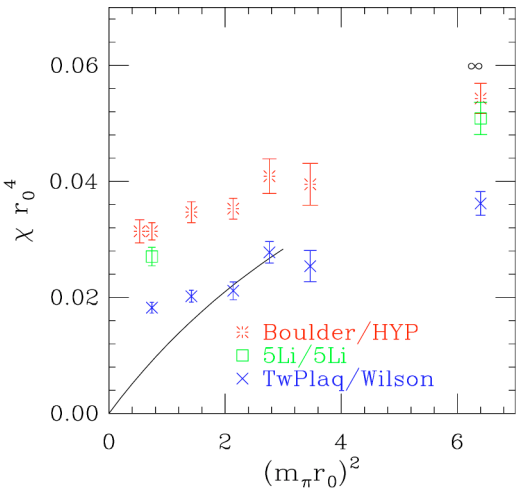

FIG. 4. Topological susceptibility vs pion mass squared in units of r_0 on the $a=0.12$ fm lattices, comparing the twisted plaquette plus Wilson method and the Boulder plus hypercubic blocking method. Also shown are two results for the 5Li/5Li method. The solid line shows the prediction of leading order chiral perturbation theory. The quenched result is shown at the extreme right. The susceptibility is measured on subvolumes, as explained in Sec. IV.

Wilson result. So the choice of operator appears to account for the largest discrepancy.

We have also measured the topological susceptibility on the companion quenched $20^3\times64$ $a=0.12$ fm ensemble using three methods and found similar inequalities: TwPlaq/Wilson gave $\chi r_0^4=0.036\,(2)$; 5Li/5Li, 0.051 (3); and Boulder/HYP, 0.054 (3).

Finally we considered the entire $20^3\times64$ dataset with $a\simeq0.12$ fm tabulated in Table I. Taking ten cools and three HYP sweeps for the comparison, we plot the result in Fig. 4. Throughout, the entire mass range the TwPlaq/Wilson susceptibility is about 2/3 of the Boulder/HYP value.

Since all three methods are expected to give the same continuum limit, as they do for quenched QCD with the Wilson plaquette action [28], the discrepancy we observe at lattice spacing $a=0.12$ fm must be due to lattice artifacts. To decide what the continuum limit is and which method is closer to it, one should do a detailed scaling study. We present results of a partial study in Sec. IV, but here attempt to interpret the differences based on our observations on smooth artificial instantons.

These discrepancies are of a magnitude that would be expected from our measurements of the charge of artificial instantons of intermediate size. The average instanton radius is expected to be ≈0.3 fm [29] or $2.3a$ on these $a=0.12$ fm lattices with significant contributions from radii as

TABLE I. Topological susceptibility vs pion mass squared in units of r_0. The result χ_V is the susceptibility computed on the full lattice volume. The result χ is computed on three subvolumes for improved statistics.

β	$am_{u,d}$	am_s	cfgs	$(m_\pi r_0)^2$	$\chi_V r_0^4$	χr_0^4
			$20^3\times64$ ($a\approx.12$ fm)			
6.76	0.007	0.050	446	0.529	0.031(2)	0.0314(20)
6.76	0.010	0.050	658	0.738	0.029(3)	0.0314(15)
6.79	0.020	0.050	486	1.420	0.033(2)	0.0345(18)
6.81	0.030	0.050	564	2.141	0.030(3)	0.0353(18)
6.83	0.040	0.050	351	2.764	0.042(4)	0.0409(30)
6.85	0.050	0.050	425	3.467	0.039(4)	0.0395(36)
8.00	∞	∞	409	∞	0.055(6)	0.0543(28)
			$28^3\times96$ ($a\approx.09$ fm)			
7.09	0.0062	0.031	534	0.646	0.0155(16)	0.0193(15)
7.11	0.0124	0.031	520	1.240	0.023(5)	0.0260(27)
7.18	0.031	0.031	500	3.145	0.043(9)	0.0351(51)
8.40	∞	∞	416	∞	0.050(5)	0.0569(26)

small as one lattice unit. From Fig. 2 where ideally $Q=1$ we see that the TwPlaq/Wilson method underestimates the charge by $Q(2.3a)=0.85$ after cooling, so one would expect an underestimation of about $0.85^2=0.7$ in the susceptibility for the average instanton. For smaller instantons the TwPlaq/Wilson method gives $Q^2(1.5a)=0.03$ after cooling, instead of one. From Fig. 3, we find a ratio of 0.58 (4) between the TwPlaq/Wilson10 and Boulder/HYP3 susceptibilities at $(m_\pi r_0)^2=0.738$. The ratio is approximately the same throughout the entire mass range. For the 5Li method we have $Q^2(2.3a)=0.96$ and $Q^2(1.5a)=0.80$. By comparison the ratio 5Li/5Li to Boulder/HYP3 is 0.87(7) at $(m_\pi r_0)^2=0.738$. Consequently, one may wonder whether the apparent agreement at $a=0.12$ fm between the TwPlaq/Wilson method and chiral perturbation theory at $2\leqslant(m_\pi r_0)^2\leqslant 3$ is the result of compensating errors.

IV. RESULTS

We measured the topological susceptibility using the Boulder/HYP method on two sets of gauge configurations generated with three flavors of light Asqtad quarks of varying masses, one set with lattice spacing ≈ 0.12 fm throughout and the other, 0.09 fm [27]. The corresponding matched quenched configurations are also included. The data sample is tabulated in Table I.

Besides measuring the susceptibility on the entire lattice volume, we increased our statistics by measuring on smaller subvolumes [30]. The probability distribution follows a Gaussian in Q with width proportional to the volume. The width is decreased as the volume is decreased, leading to the same relative error in the determination of the susceptibility for the same sample size on the smaller volume. To the extent that the subvolume measurements are uncorrelated, the sample is effectively increased by a factor equal to the number of subdivisions, so the error should decrease by the square root of this number. This process cannot be continued indefinitely, since we should eventually discover strong correlations among adjacent subvolumes.

Measuring the susceptibility on subvolumes may even be indicated for actions and updating algorithms that give persistent global charge, but fluctuating local charge densities.

Accordingly, we divided the lattices along the time dimension into three hypercubic subvolumes mostly separated by a small unused space. For the $28^3\times 96$ lattices these subvolumes of size 28^4 were constructed from imaginary time ranges [0,27], [32,59], and [64,91], and for the $20^3\times 64$ lattices of size 20^4 from time ranges [0,19], [22,41], and [44,63]. Since the boundary condition on the subvolume is not periodic, this practice splits instantons. However, the rms charge in the subvolumes (in the range $4<|Q|<7$) seems large enough to ensure that the boundary effects are not significant.

We measured the correlations in the topological charge history between charges in different subvolumes. That is, if we denote by Q_{uk} the charge measured in subvolume u on gauge configuration k in a data sample with N gauge field configurations, we define the correlation coefficient to be

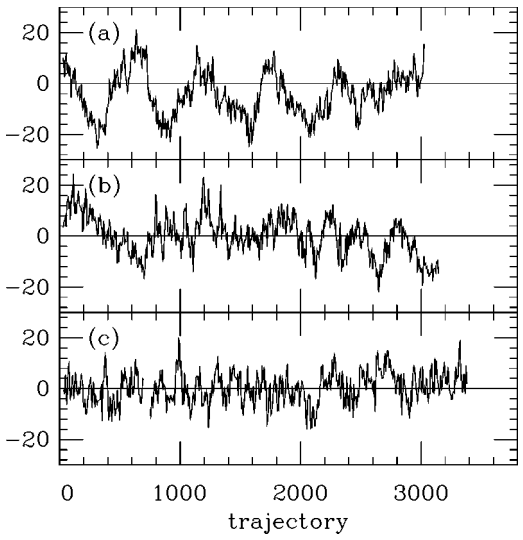

FIG. 5. Full volume topological charge after three HYP sweeps vs molecular dynamics trajectory for the $28^3\times 96$ dataset with (a) $am_{u,d}=am_s=0.031$, (b) $am_{u,d}=0.0124$, $am_s=0.031$, and (c) $am_{u,d}=0.0062$, $am_s=0.031$. In the last case two separate time series are plotted with the second starting after the break at 700 trajectories.

$$c_{uv}=\frac{1}{N}\sum_k Q_{uk}Q_{vk}/(|Q_u||Q_v|) \tag{5}$$

where $|Q_u|=\sqrt{\langle Q_u^2\rangle}$ is the rms charge on the subvolume u. The 33 correlation coefficients for our entire dataset are roughly Gaussian distributed about zero with a mean of -0.004 and width of 0.09. Thus we feel confident that we may treat the subvolume measurements as statistically independent observations.

The measurements are clearly correlated in Monte Carlo time. The Asqtad dynamical lattices were saved every sixth molecular dynamics trajectory. The $20^3\times 64$ quenched lattices were saved every tenth quasi-heatbath sweep and the $28^3\times 96$ every 50th. We made charge measurements on all available lattices. A particularly striking example is given by the time history for the total charge on the $28^3\times 96$ lattice with three degenerate quark masses $am_{u,d}=am_s=0.31$, as shown in the upper panel of Fig. 5 [17]. The horizontal scale counts molecular dynamics trajectories. Time histories for the subvolume charges for the same dataset are shown in Fig. 6 where the prominent oscillations are much less evident. Other time histories shown in the lower two panels of Fig. 5 do not show such a striking effect. On the $28^3\times 96$ datasets the autocorrelation length, measured on the subvolumes by summing the autocorrelation coefficient, ranges from approximately 10 trajectories for $am_{u,d}=0.0062$ to 35 trajectories at $am_{u,d}=0.031$. Charge measurements on the corresponding quenched lattices are only slightly correlated. On the coarser $20^3\times 64$ lattices we find weaker autocorrelation, but still roughly monotonically increasing with quark mass from fewer than six trajectories at $am_{u,d}=0.007$ to ten trajectories at $am_{u,d}=0.050$. This trend appears to be contrary to some expectations [31].

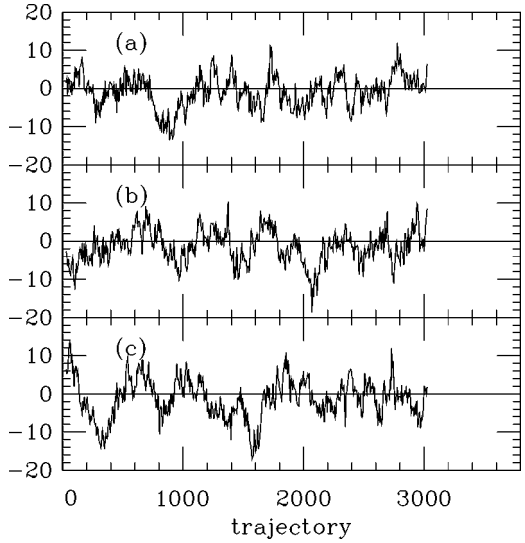

FIG. 6. Same as Fig. 5(a), but measured on three 28^4 subvolumes defined by time slices (a) [0,27], (b) [32,59] and (c) [64,91].

The autocorrelations in topological charge found with the Asqtad action and $2+1$ flavors of quarks appear to be longer than those found with the conventional thin link staggered fermion action and two flavors. Shown in Fig. 7 is a comparison of the topological charge history from the ensemble of Fig. 5(b) and an ensemble generated with the conventional unimproved thin-link staggered fermion algorithm [32]. These simulations were done at approximately the same value of $(m_\pi r_0)^2$ (unimproved 1.06, improved 1.23) and lattice spacing (unimproved 0.10 fm, improved 0.09 fm). It is apparent that the configurations decorrelate less rapidly with the improved action and extra flavor.

Statistical errors in the topological susceptibility are determined by taking the larger of the error corrected for autocorrelations and the error obtained by extrapolating to infinite bin size.

We have measurements of the topological susceptibility at two lattice spacings. Thus we may venture an extrapolation to the continuum limit. This is done by first interpolating in

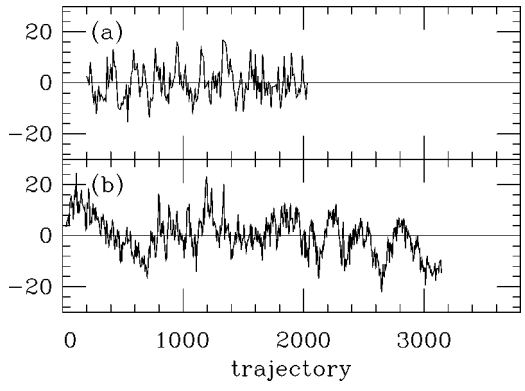

FIG. 7. (a) Topological charge after three HYP sweeps vs molecular dynamics trajectory for the conventional unimproved staggered fermion action on a $24^3\times 64$ dataset with two degenerate quark flavors $am_{u,d}=0.01$, compared with (b) the result from the Asqtad action from Fig. 5(b).

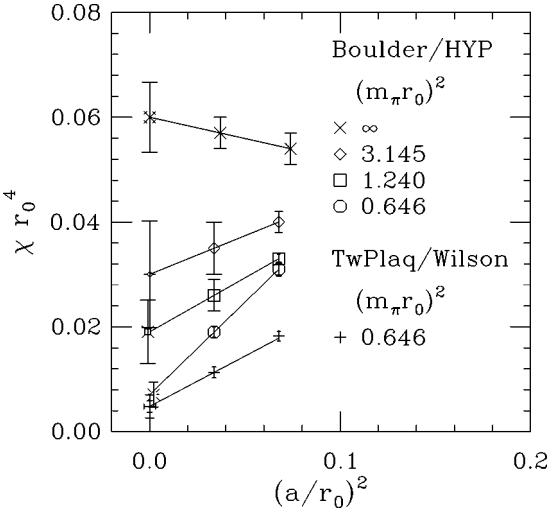

FIG. 8. Continuum extrapolation of the topological susceptibility found with the Boulder/HYP and for the lightest quark mass the TwPlaq/Wilson methods.

$(r_0 m_\pi)^2$ the topological susceptibility on the coarse lattice to the three pion mass values where we have measurements on the finer lattice. We then do a linear extrapolation at fixed $(m_\pi r_0)^2$ to zero a^2/r_0^2 as shown in Fig. 8. We see that the quenched susceptibility rises with decreasing lattice spacing, but falls for the unquenched lattices with a slope that increases with quark mass.

We have done a comparable extrapolation using the TwPlaq/Wilson method, but with only one of the $a=0.09$ fm dynamical ensembles. Results are also shown in Fig. 8. Within the limitations of these few points, we find satisfactory agreement between the extrapolated values found with both methods.

Our main results for the topological susceptibility are summarized in Table I and Fig. 9. We see that within errors the continuum extrapolation gives reasonable agreement with the prediction of leading order chiral perturbation theory, Eq. (4).

V. DISCUSSION

The combined effect of the discretization artifacts discussed in Sec. III A is that, depending on the method of measurement, the lattice topological susceptibility $\hat{\chi}$ is both additively and multiplicatively renormalized relative to the continuum value χ [9,34]:

$$\hat{\chi}(a,m_q)=M(a,m_q)^2\chi(m_q)+A(a,m_q), \tag{6}$$

where we understand the susceptibilities to be expressed in some appropriate choice of physical units. Having some indication of the scaling behavior of these methods, we suggest a scenario for the behavior of the functions M and A in Eq. (6).

To suppress the ultraviolet fluctuations prior to measuring the topological charge, it is necessary to smooth the gauge configurations. In the quenched theory, smoothing eventually drives A to 0. However, since fluctuations involving instan-

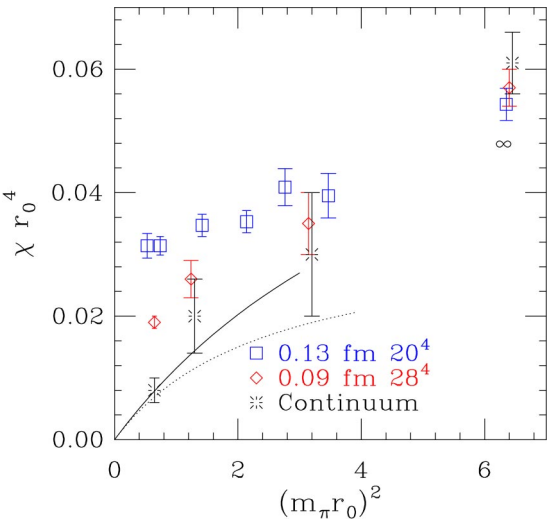

FIG. 9. Topological susceptibility vs pion mass squared in units of r_0 with dynamical Asqtad quarks. The solid line shows the prediction of leading order chiral perturbation theory. The dotted line gives a phenomenological proposal for nonperturbative behavior [33]. The quenched result is shown at the extreme right.

tons of sizes at or below the cutoff are always missed, one expects $M<1$, at least for operators that do not overestimate the charge of small instantons. Therefore, $\hat{\chi}^{(\mathrm{qu})}<\chi^{(\mathrm{qu})}$. Indeed, we see from Fig. 4 and the continuum extrapolation in Fig. 8 that at $a=0.12$ fm all three methods underestimate the quenched susceptibility.

In full QCD the virtual fermions screen the topological charge, but they screen everything they see, including dislocations. Smoothing removes dislocations and small instantons; those that are not involved in the screening of more extended topological charges do not cause trouble, but those that are leave behind the more extended (and now less screened) charges that are relatively stable under smoothing. This effect increases the susceptibility and shows up as an anomalous A that does not vanish with continued smoothing.

As we take the continuum limit in full QCD, we expect $M\rightarrow 1$, as in the quenched case, and also $A\rightarrow 0$, as the lattice action, combined with smoothing, gradually suppresses dislocations. The two trends act in opposite directions; to decide which dominates, we must consider the quark mass dependence. There are two regimes. The first is for large m_q, where M dominates and A is small. In this ''instanton-dominated'' region, the behavior is similar to the quenched theory, and discretization effects lead to an underestimate $\hat{\chi}(a,m_q)<\chi(m_q)$ at nonzero a. On the other hand, at small quark mass the continuum susceptibility is small. The factor M is expected to depend only weakly on m_q, so the lattice measurement is dominated by A. In this ''dislocation-dominated'' regime there is likely to be an enhancement $\hat{\chi}(a,m_q)>\chi(m_q)$ at nonzero a. Indeed, from Fig. 4 and the continuum extrapolations at $(m_\pi r_0)^2=0.646$ and infinity in Fig. 8 we see that at $a=0.12$ fm all three methods overestimate the susceptibility expected at the nearby point $(m_\pi r_0)^2=0.738$ and underestimate it at infinite quark mass. With the Boulder/HYP method, our results suggest that the scaling slope decreases as the quark mass is increased.

Given that the mean gauge action decreases by orders of magnitude under smoothing at $a\simeq 0.1$ fm, it is reasonable to assume that dislocations are abundant and participate significantly in screening more extended topological charges. Erasing them then contributes to A. The number of instantons is not a strong function of quark mass. (The Wilson gauge action after 20 cooling sweeps is dominated by instantons, so gives a measure of their number. We find that the mean action density on the coarse lattices varies by less than 10% across the dynamical and quenched ensembles in this study.) We thus expect A to vary at most weakly with the quark mass in the dislocation-dominated region of quark mass. Our results for the $a=0.12$ fm lattices plotted in Fig. 4 show that for all methods the susceptibility levels off below $(m_\pi r_0)^2 \simeq 2$.

But leveling off can also be attributed to shortcomings of the lattice fermion formulation itself. The would-be zero modes of the staggered lattice Dirac matrix are not at exactly zero. If the deviation is comparable to the virtual quark mass, some of the topological modes are not properly screened. Consequently, $\hat{\chi}(a,m_q)$ does not vanish as it should as the quark mass is reduced. The chiral limit is then governed by the dependence of A on m_q.

VI. CONCLUSIONS

We have measured the topological susceptibility on lattices generated with Asqtad improved staggered fermions of varying mass and two lattice spacings, $a=0.12$ fm and $a=0.09$ fm. We have compared three methods for measuring the topological charge on these lattices and selected the Boulder method with hypercubic blocking, since it appears best capable at these lattice spacings of preserving small instantons. We show in one comparison at $a=0.12$ fm that the largest difference between the Boulder/HYP and TwPlaq/Wilson methods can be attributed to the operator, rather than the smoothing method. We find that at both lattice spacings there is clear evidence that dynamical quarks suppress topological fluctuations and the suppression increases with decreasing quark mass and with decreasing lattice spacing. However, at fixed nonzero lattice spacing, lattice artifacts at small quark masses are still substantial, and the susceptibility does not decrease as expected from chiral perturbation theory at small quark masses. Nevertheless, an $O(a^2)$ extrapolation of our data to zero a gives results that are consistent with the leading order prediction. Within the limitations of our statistics, this is the first study to show satisfactory agreement with the predictions of chiral perturbation theory at quark masses much smaller than the strange quark mass.

ACKNOWLEDGMENTS

We are grateful to Philippe de Forcrand for providing us his computer code for the 5Li/5Li measurements. Computations were performed at LANL, NERSC, NCSA, ORNL,

PSC, SDSC, FNAL, the CHPC (Utah), the Indiana University SP and the Netra cluster (University of the Pacific). This work is supported by the U.S. National Science Foundation under grants PHY01-39929 and PHY00-98395 and the U.S. Department of Energy under contracts DE-FG02-91ER-40628, DE-FG03-95ER-40894, DE-FG02-91ER-40661, and DE-FG03-95ER-40906. A.H. is supported by the Royal Society.

[1] K. Orginos and D. Toussaint, Phys. Rev. D **59**, 014501 (1999); K. Orginos, D. Toussaint, and R.L. Sugar, *ibid.* **60**, 054503 (1999); G.P. Lepage, *ibid.* **59**, 074502 (1999).
[2] C. Bernard *et al.*, Phys. Rev. D **64**, 054506 (2001).
[3] HPQCD, UKQCD, MILC, and Fermilab Collaborations, C.T. Davies *et al.*, hep-lat/0304004.
[4] F. Knechtli and A. Hasenfratz, Phys. Rev. D **63**, 114502 (2001); A. Hasenfratz and F. Knechtli, Comput. Phys. Commun. **148**, 81 (2002).
[5] D.B. Kaplan, Phys. Lett. B **288**, 342 (1992); Nucl. Phys. B (Proc. Suppl.) **30**, 597 (1992); Y. Shamir, Nucl. Phys. **B406**, 90 (1993); V. Furman and Y. Shamir, *ibid.* **B439**, 54 (1995)
[6] H. Neuberger, Phys. Lett. B **417**, 141 (1998); H. Neuberger, Phys. Rev. Lett. **81**, 4060 (1998).
[7] T. DeGrand, A. Hasenfratz, and T.G. Kovacs, Nucl. Phys. **B505**, 417 (1997).
[8] A. Hasenfratz and F. Knechtli, Phys. Rev. D **64**, 034504 (2001).
[9] P. Di Vecchia, K. Fabricius, G.C. Rossi, and G. Veneziano, Nucl. Phys. **B192**, 392 (1981); M. Peskin, Ph.D. thesis, 1978.
[10] M. Teper, Phys. Lett. **162B**, 357 (1985); E.M. Ilgenfritz, M.L. Laursen, G. Schierholz, M. Muller-Preussker, and H. Schiller, Nucl. Phys. **B268**, 693 (1986); J. Hoek, Phys. Lett. **166B**, 199 (1986).
[11] P. de Forcrand, M. Garcia Perez, and I.O. Stamatescu, Nucl. Phys. B (Proc. Suppl.) **47**, 777 (1996); Nucl. Phys. **B499**, 409 (1997).
[12] CP-PACS Collaboration, A. Ali Khan *et al.*, Phys. Rev. D **64**, 114501 (2001).
[13] A. Hasenfratz, Phys. Rev. D **64**, 074503 (2001).
[14] UKQCD Collaboration, A. Hart and M. Teper, Phys. Lett. B **523**, 280 (2001); UKQCD Collaboration, C.R. Allton *et al.*, Phys. Rev. D **65**, 054502 (2002); UKQCD Collaboration, A. Hart and M. Teper, hep-ph/0004180.
[15] B. Alles, M. D'Elia, and A. Di Giacomo, Nucl. Phys. B (Proc. Suppl.) **83**, 431 (2000); B. Alles, M. D'Elia, and A. Di Giacomo, Phys. Lett. B **483**, 139 (2000); CP-PACS Collaboration, A. Ali Khan *et al.*, Nucl. Phys. B (Proc. Suppl.) **83**, 162 (2000); TXL Collaboration, G.S. Bali *et al.*, Phys. Rev. D **64**, 054502 (2001).
[16] Kovacs found promising results with the overlap action, but because of the prohibitive cost, drastic approximations to the action and ensembles were required. T.G. Kovacs, hep-lat/0111021; Nucl. Phys. B (Proc. Suppl.) **106**, 578 (2002).
[17] MILC Collaboration, C. Bernard *et al.*, Nucl. Phys. B (Proc. Suppl.) **119**, 991 (2003)
[18] R.J. Crewther, Phys. Lett. **70B**, 349 (1977); P. Di Vecchia and G. Veneziano, Nucl. Phys. **B171**, 253 (1980).
[19] H. Leutwyler and A. Smilga, Phys. Rev. D **46**, 5607 (1992).
[20] S. Dürr, Nucl. Phys. **B611**, 281 (2001).
[21] C. Bernard *et al.*, Nucl. Phys. B (Proc. Suppl.) **119**, 257 (2003).
[22] A. Hasenfratz and C. Nieter, Phys. Lett. B **439**, 366 (1998).
[23] MILC Collaboration, C. Bernard *et al.*, Nucl. Phys. B (Proc. Suppl.) **119**, 769 (2003); see also UKQCD Collaboration, A. Hart, *ibid.* **106**, 575 (2002).
[24] A. Hasenfratz, Phys. Rev. D **64**, 074503 (2001).
[25] M. Falcioni, M.L. Paciello, G. Parisi, and B. Taglienti, Nucl. Phys. **B251**, 624 (1985); APE Collaboration, M. Albanese *et al.*, Phys. Lett. B **192**, 163 (1987).
[26] R. Sommer, Nucl. Phys. **B411**, 839 (1994).
[27] The Asqtad lattice ensembles in this study are slightly expanded versions of the datasets described in previous work and publicly available at the Department of Energy National Energy Research Scientific Computing Center (NERSC) Gauge Connection URL http://qcd. nersc. gov. See Ref. [21] and C.W. Bernard *et al.*, Phys. Rev. D **64**, 054506 (2001).
[28] For a review, see M. Teper, Nucl. Phys. B (Proc. Suppl.) **83**, 146 (2000).
[29] E.V. Shuryak and T. Schafer, Annu. Rev. Nucl. Part. Sci. **47**, 359 (1997).
[30] P. de Forcrand, M. Garcia-Perez, J. E. Hetrick, E. Laermann, J. F. Lagae, and I. Stamatescu, Nucl. Phys. B (Proc. Suppl.) **73**, 578 (1999).
[31] G. Boyd, B. Alles, M. D'Elia, and A. Di Giacomo, hep-lat/9711025.
[32] MILC Collaboration, C.W. Bernard *et al.*, Nucl. Phys. B (Proc. Suppl.) **63**, 215 (1998).
[33] The results of [20] can be extended to three flavors, using $1/\chi = 1/\chi_{\mathrm{LO}} + 1/\chi_{\mathrm{quenched}}$. S. Dürr, private communication (2003).
[34] M. Campostrini, A. Di Giacomo, and H. Panagopoulos, Phys. Lett. B **212**, 206 (1988); A.S. Kronfeld, Nucl. Phys. B (Proc. Suppl.) **4**, 329 (1988).